THE JOURNAL OF BIOLOGICAL CHEMISTRY VOL. 285, NO. 40, pp. 30779–30791, October 1, 2010

Deletions and Mutations in the Acidic Lipid-binding Region of the Plasma Membrane Ca^{2+} Pump

*A STUDY ON DIFFERENT SPLICING VARIANTS OF ISOFORM 2**

Received for publication, May 3, 2010, and in revised form, July 19, 2010 Published, JBC Papers in Press, July 19, 2010, DOI 10.1074/jbc.M110.140475

Marisa Brini[‡1], Francesca Di Leva[‡§], Claudia K. Ortega[¶], Teuta Domi[‡§], Denis Ottolini[‡§], Emanuela Leonardi[‖], Silvio C. E. Tosatto[‖], and Ernesto Carafoli[¶]

From the Departments of [‡]Biological Chemistry and [§]Experimental Veterinary Sciences, University of Padova, 35131 Padova, the [¶]Venetian Institute of Molecular Medicine, 35129 Padova, and the [‖]Department of Biology, University of Padova, 35131 Padova, Italy

Acidic phospholipids increase the affinity of the plasma membrane Ca^{2+}-ATPase pump for Ca^{2+}. They interact with the C-terminal region of the pump and with a domain in the loop connecting transmembrane domains 2 and 3 (A_L region) next to site A of alternative splicing. The contribution of the two phospholipid-binding sites and the possible interference of splicing inserts at site A with the regulation of the ATPase activity of isoform 2 of the pump by phospholipids have been analyzed. The activity of the full-length *z/b* variant (no insert at site A), the *w/b* (with insert at site A), and the *w/a* variant, containing both the 45-amino acid A-site insert and a C-site insert that truncates the pump in the calmodulin binding domain, has been analyzed in microsomal membranes of overexpressing CHO cells. The A-site insertion did not modify the phospholipid sensitivity of the pump, but the doubly inserted *w/a* variant became insensitive to acidic phospholipids, even if containing the intact A_L phospholipid binding domain. Pump mutants in which 12 amino acids had been deleted, or single lysine mutations introduced, in the A_L region were studied by monitoring agonist-induced Ca^{2+} transients in overexpressing CHO cells. The 12-residue deletion completely abolished the ATPase activity of the *w/a* variant but only reduced that of the *z/b* variant, which was also affected by the single lysine substitutions in the same domain. A structural interpretation of the interplay of the pump with phospholipids, and of the mechanism of their activation, is proposed on the basis of molecular modeling studies.

The plasma membrane Ca^{2+}-ATPases (PMCAs)[2] extrude Ca^{2+} from cells, maintaining the resting level of intracellular Ca^{2+} and controlling the Ca^{2+} transients induced by agonists. Four basic PMCA isoforms are encoded by four independent genes. *PMCA1* and *-4* are ubiquitously expressed, whereas *PMCA2* and *-3* are restricted to brain, muscles, and few other tissues; the tissue-restricted isoforms are more active in exporting Ca^{2+} than the ubiquitous isoforms (1), probably due to their higher affinity for the activator calmodulin. The transcript of each gene is subjected to alternative splicing at sites A and C. About 30 splice variants have so far been detected at the RNA or protein levels (2).

The architecture of the PMCAs predicts 10 transmembrane domains, two large intracellular loops, and N- and C-terminal cytoplasmic tails. The 90-residue N-terminal portion appears not to have specific functions even if it contains a consensus binding site for the 14-3-3 protein, which inhibits three of the four pump isoforms (3, 4). The cytosolic loop between transmembrane domains 2 and 3 contains a site that binds activatory acidic phospholipids and site A of alternative splicing upstream of it. Pump variants containing the A-splice site insert are targeted to the apical plasma membrane (5), and the insert has recently been suggested to have a role in the interactions of the pump with lipids in the plasma membrane (6). The C-terminal tail contains other regulatory sites of the pump, among them the positively charged calmodulin binding domain, which also binds acidic phospholipids (7), the consensus sites for protein kinases A (PKA, isoform-specific) and C (PKC), and high affinity allosteric Ca^{2+}-binding sites.

Under nonactivated conditions, the C-terminal tail of the pump is proposed to fold over to interact with two sites in the first and second cytosolic loops of the enzyme, compromising the access to the active center. Calmodulin then interacts with its binding domain, removing it from its docking sites next to the active center and freeing the pump from autoinhibition.

The calmodulin regulation of the pump has been extensively investigated and is now well understood but that mediated by acidic phospholipids is still unclear. Acidic phospholipids enhance the Ca^{2+} sensitivity of the PMCA to a greater extent than calmodulin (8–11). The order of stimulatory potency (phosphatidylinositol 4,5-biphosphate > phosphatidylinositol 4-phosphate > phosphatidylinositol ~ phosphatidylserine (PS) ~ phosphatidic acid) is proportional to the number of negative charges on the lipids (12). The stimulation is appreciably reduced by complexing the negative charges with polyamines or neomycin (13). Recently, diacylglycerol has also been shown to be a stimulator of the PMCA. Interestingly, the activation induced by diacylglycerol is additional to that produced by calmodulin and PKC, suggesting that diacylglycerol interacts with the PMCA through a specific mechanism (14).

* This work was supported by the Telethon Foundation Project GGP04169 (to M. B.), the Italian Ministry of University and Research PRIN 2003 and 2005 (to M. B.), and by the FP6 Program of the European Union, FP6 Integrated Project EUROHEAR, LSHG-CT-20054-512063 (to E. C.).

[1] To whom correspondence should be addressed: Dept. of Biological Chemistry, University of Padova, Viale G. Colombo, 3, 35131 Padova, Italy. Tel.: 39-049-8276150; Fax: 39-049-8276125; E-mail: marisa.brini@unipd.it.

[2] The abbreviations used are: PMCA, plasma membrane Ca^{2+}-ATPase; PS, phosphatidylserine; PDB, Protein Data Bank; CaM, calmodulin.

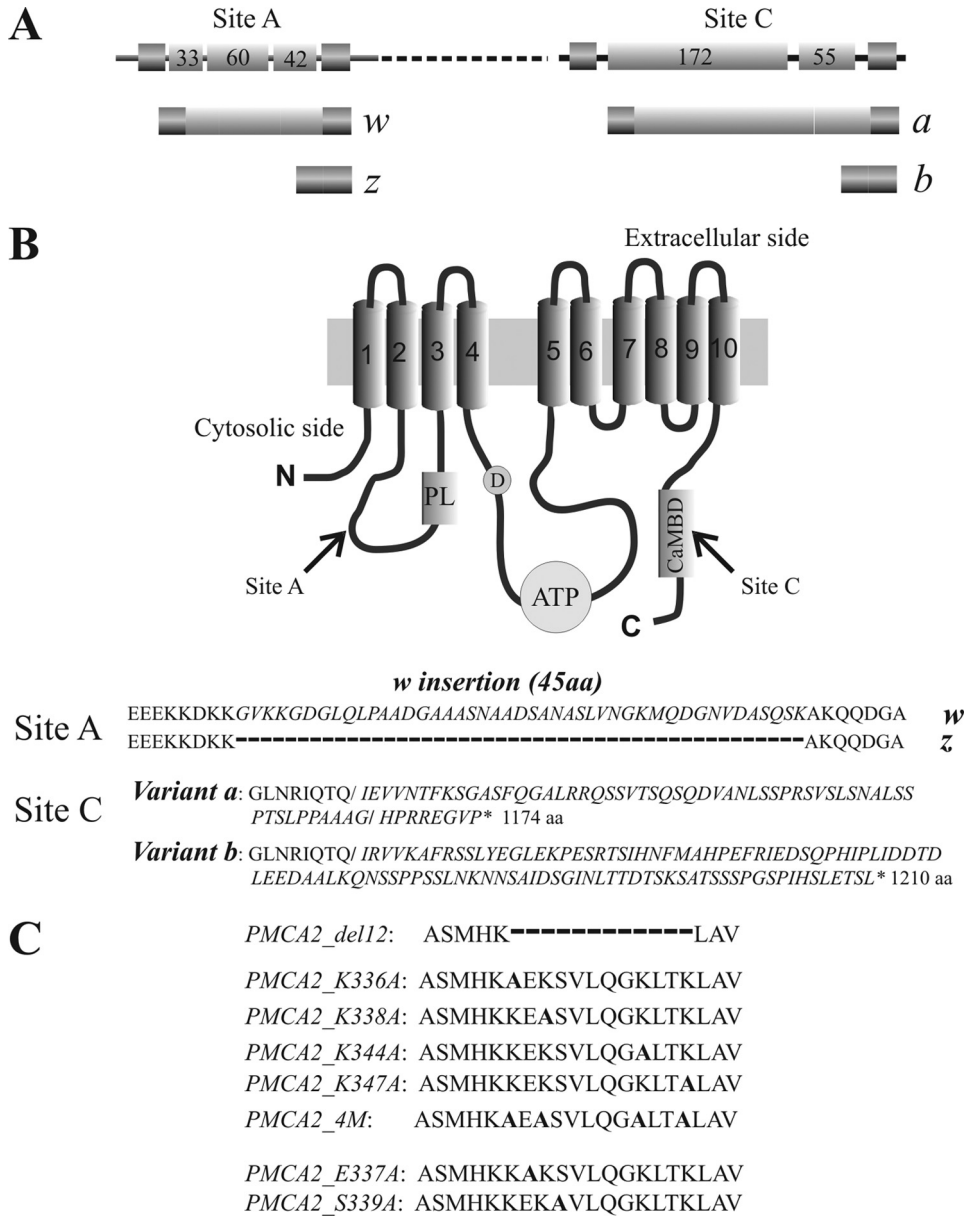

FIGURE 1. *A,* linear representation of the alternative splicing options at site A and site C of the PMCA2 transcript. Exons are indicated by *shadow boxes* and introns by the *black line*. The *numbers* in the *boxes* represent the nucleotide number of each exon. *B,* topography model of the plasma membrane Ca^{2+}-ATPase and sequences of alternative splicing products of isoform 2. The 10 putative transmembrane domains are *numbered* and indicated by *shadow boxes*. *PL* indicates the phospholipid binding domain downstream of site A of alternative splicing; *D* indicates the catalytic aspartate; *ATP* and *CaMBD* indicate the ATP-binding site and the calmodulin binding domain, which contains site C of alternative splicing. *C,* sequences of the PMCA2 region that have been mutated or deleted in the constructs used in this study. The alanine that replaces the mutated residue in the different constructs is indicated in *bold*. The *dashed line* represents the 12 amino acids deletion.

The acidic phospholipid-binding region next to splice A was recently deleted in a variant of PMCA4 containing an inserted exon at splicing site A (variant *xb*) (15, 16). Partial deletions did not alter Ca^{2+} transport activity but made the pump insensitive to acidic phospholipids. However, complete removal of the domain made the pump inactive (15).

The contributions of the two phospholipid-binding sites, and of the alternative splicing at site A next to one of them, to the regulation of the pump have not been analyzed. It was interesting to study these aspects on isoform 2 of the pump, as this isoform has very high activity even in the absence of calmodulin (17, 18), but it responds to acidic phospholipids in the same way as PMCA4 (17). In addition, the splicing mechanisms of PMCA2 generate a larger number of variants than in other isoforms; up to three exons are inserted at site A, generating variant *z* (no exons included), variant *y* (two exons included), variant *x* (one exon included), and variant *w* (all three exons included). Splicing at site C excludes two novel exons (variant *b*, full length) or includes them (variant *a*). The *a* insertion leads to a truncated version of the pump that only contains about half of the original calmodulin binding domain (17, 18). We had previously reported that the *z/a* and *w/b* PMCA2 variants behaved essentially as the full-length, non-inserted, (*z/b*) pump (perhaps, they were slightly less efficient) (1, 19, 20). The doubly inserted *w/a* PMCA2 variant had only limited ability to rapidly increase activity when challenged with a Ca^{2+} pulse but had about the same highly nonstimulated (basal) activity of the full-length *z/b* variant (19).

This contribution explores the activation of splicing variants of isoform 2 of the PMCA pump by acidic phospholipids. Because the negative charges on the lipids are likely to be important in the stimulatory effect, the study was performed using a pump variant in which a 12-residue stretch in the A_L acidic phospholipid binding domain, which contains four positively charged residues, was removed. Point mutations that selectively substituted positive residues (Lys), or two other conserved polar residues (Ser and Glu), were also introduced in the stretch. The scheme of Fig. 1 summarizes graphically the details of the PMCA2 variants and mutants used in this study.

EXPERIMENTAL PROCEDURES

Cell Cultures and Transfection—CHO cells were cultured in Ham's F-12 nutrient mixture (Invitrogen), supplemented with 10% fetal bovine serum (FBS), 2 mM glutamine, penicillin (60 μg/μl), and streptomycin (120 μg/μl) in 75-cm^2 Falcon flasks at

37 °C. For the microsomes preparation, CHO cells were plated on 150 × 25-mm Petri dishes, allowed to grow to 50% confluence, and transfected according to a calcium-phosphate procedure with 30 μg of total plasmid DNA. For the aequorin and immunocytochemistry experiments, CHO cells were plated onto 13-mm glass coverslips, allowed to grow to 50% confluence, and transfected according to a calcium-phosphate procedure with 3 μg of total plasmid DNA or with 1.5 μg of each plasmid DNA in the case of co-transfection. GFP-tagged PMCA2 *z/b* and *w/b* are of human origin, and GFP-tagged PMCA2 *w/a* variants (WT and del12 mutant) are from rat. Untagged PMCA2 pump variants (*w/a* and *z/b*) of human origin were also used in the Ca^{2+} measurements of experiments in living cells. No differences were observed between the GFP-tagged and -untagged PMCA2 activity.

The average transfection efficiency approached 25%, and the increase of PMCA protein in overexpressing cells, calculated by densitometric analysis of Western blotting showing the endogenous PMCA (*i.e.* blots developed with the monoclonal antibody 5F10 that recognized all PMCA isoforms) and corrected for the whole cell population, would correspond to about 3-fold the endogenous level (data not shown).

Microsomal Membrane Preparations from CHO Cells—Cells from five 150 × 25-mm dishes were washed once with phosphate buffered saline (PBS) containing 1 mM EDTA and harvested in 10 ml of PBS containing 0.1 mM phenylmethylsulfonyl fluoride (PMSF) and a mixture of EDTA-free protease inhibitors (Roche Applied Science). Cells were collected by centrifugation (2000 × *g*, 10 min) at 4 °C and resuspended in 6 ml of a hypotonic solution of 10 mM Tris-HCl, pH 7.5, 1 mM $MgCl_2$, 0.1 mM PMSF, a mixture of EDTA-free protease inhibitors, and 2 mM dithiothreitol (DTT). The cells were swollen for 15 min on ice and then subjected to three cycles of freeze and thaw. The homogenate was diluted with an equal volume of 0.5 M sucrose, 0.3 M KCl, 2 mM dithiothreitol, 10 mM Tris-HCl, pH 7.5, homogenized again with three cycles of freeze and thaw, and centrifuged at 5000 × *g* for 15 min. KCl was added up to 0.6 M in the supernatant, and to remove calmodulin, an excess of EDTA (1.5 mM) was also added. The suspension was centrifuged at 100,000 × *g* for 40 min to pellet the microsomal fraction. The final pellet was resuspended in a solution containing 0.25 M sucrose, 0.15 M KCl, 10 mM Tris-HCl, pH 7.5, 2 mM DTT, and 20 μM $CaCl_2$, at a protein concentration of 1–3 mg/ml, and stored in liquid N_2.

ATPase Activity Assay—The ATPase activity was measured by the coupled enzyme assay (modified from Ref. 21) monitoring the absorbance of NADH at 340 nm. The decrease in A_{340} can be converted into ATPase activity where one molecule of NADH oxidized to NAD^+ corresponds to the production of one molecule of ADP by the ATPase. The assay was carried out at 37 °C in a final volume of 1 ml of a mixture containing 20 mM Tris-HCl, pH 7.2, 5 mM $MgCl_2$, 0.5 mM EGTA, 0.1 M KCl, 0.5 mM phosphoenolpyruvate, 0.15 mM NADH, 1.4 units of pyruvate kinase/lactic dehydrogenase (Roche Applied Science), 4 mM ATP, 25 μg of PMCA membranes, and 50 μM $CaCl_2$. The ATPase activity, detected at 340 nm (DU640 Spectrophotometer, Beckman Coulter), was expressed in micromoles of P_i/min/mg of protein (moles of phosphate originated from the ATP hydrolysis); the maximal activity and the basal activity were calculated by multiplication of the activity curve slope value by a factor considering the NADH molar extinction coefficient (ϵ_{NADH}) and the amount of protein (in micrograms). The real activity was obtained subtracting the basal activity from the maximal activity. The assay was performed in the presence of 5 μg/ml oligomycin and 0.1 μM thapsigargin. To test calmodulin (CaM) or phosphatidylserine (PS) activation of the pump, 200 nM CaM or 25 μM PS was preincubated with the membranes for 5 min at 37 °C before starting the assay.

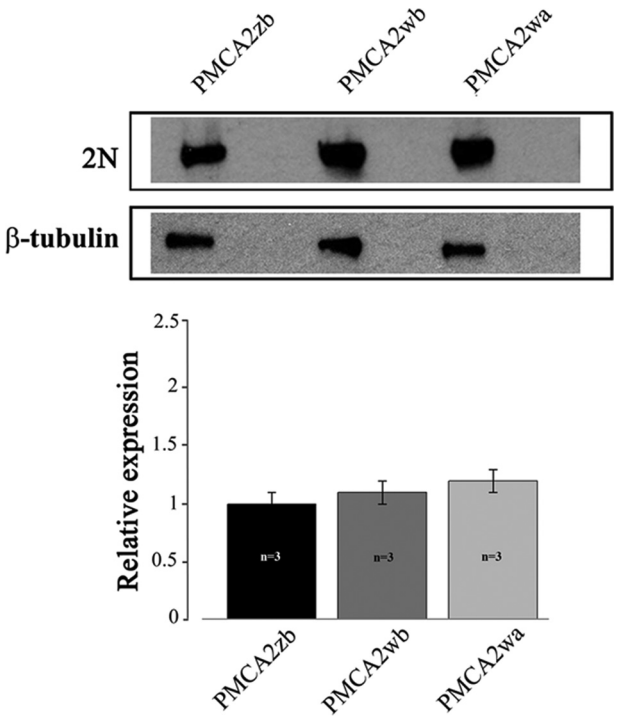

FIGURE 2. **Western blotting and densitometric analysis of PMCA2 isoform overexpression in transfected CHO cells.** 20 μg of crude membrane proteins from transfected CHO cells, prepared by a freeze and thaw method, were separated by SDS-PAGE as described under "Experimental Procedures" and stained with polyclonal antibody 2N, which recognizes isoform 2 of the pump or against tubulin. The lanes correspond to cells transfected with the indicated variants of PMCAs fused to GFP. The data are representative of at least three independent experiments.

Generation of PMCA2z/b_del12 and PMCA2z/b Mutant Expression Plasmids—To generate PMCA2*z/b* with the deletion of 12 amino acids in the domain that binds acidic phospholipids, two PCR amplification products that did not contain the portion of 12 amino acids were generated using four different primers bearing restriction sites for EcoRI/HindIII and HindIII/BamHI as follows: 5′-cgg<u>GAATTC</u>**atg**ggtgacatgaccaac-3′; 5′-cgg<u>TTCGAA</u>gtgcatgctggccttcct-3′; 5′-cgg<u>TTCGAA</u>gctgtgcagatcgggaag-3′; cgg<u>GGATCC</u>ctaaagcgacgtctccag. The PCR products were digested with the respective restriction enzymes and were inserted in a three-part ligation reaction in pcDNA3 vector (Invitrogen) digested with EcoRI and BamHI. The construct was controlled by sequencing.

In vitro site mutagenesis in the PMCA2*z/b* was carried out with QuikChange II site-directed mutagenesis kit (Stratagene) according to the manufacturer's instructions using the following primers: Lys-336 sense 5′-ccagcatgcacaag**GC-**

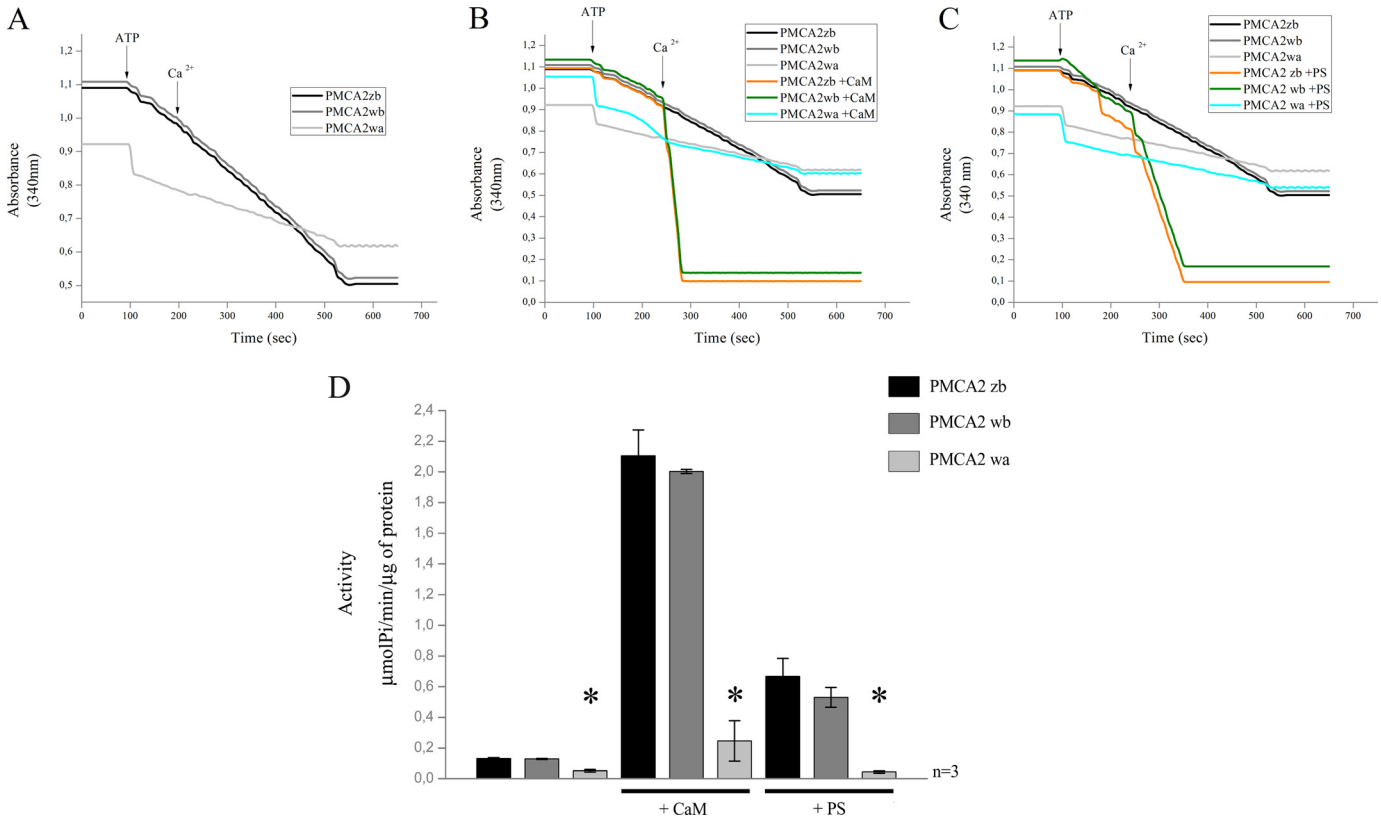

FIGURE 3. *A,* comparison of Ca^{2+} transport activity measured on microsomal membranes isolated from CHO cells overexpressing PMCA2 *z/b*, *w/b,* and *w/a* variants. Membranes vesicles were preincubated at 37 °C, and Ca^{2+} uptake was initiated by the addition of 4 mM ATP (where indicated). 50 μM $CaCl_2$ was added where indicated. *B,* CaM dependence of Ca^{2+} uptake by microsomal membranes preincubated at 37 °C with 200 nM CaM. *C,* acidic phospholipid (PS) dependence of Ca^{2+} uptake by microsomal membranes preincubated at 37 °C with 25 μM PS. *A–C,* ATPase activity was indicated as the decrease of the absorbance at 340 nm. *D, histograms* show the means ± S.D. of the activity of the pumps. The activity was expressed as micromoles of P_i/min/μg of protein and calculated as indicated under "Experimental Procedures." The data are representative of at least three experiments with different membranes preparations. *, $p < 0.05$, in respect to the respective controls in the absence of CaM and PS.

ggagaagtccgtgc-3′ and antisense 5′-gcacggacttctcc**GC**cttgtgcatgctgg-3′; Lys-338 sense 5′-tgcacaagaaggag**GC**gtccgtgctgcagg-3′ and antisense 5′-cctgcagcacggac**GC**ctccttcttgtgca-3′; Lys-344 sense 5′-cgtgctgcagggc**GC**gctcaccaagctg-3′ and antisense 5′- cagcttggtgagc**GC**gccctgcagcacg-3′; Lys-347 sense 5′-gggcaagctcacc**GC**gctggctgtgcagat-3′ and antisense 5′-atctgcacagccagc**GC**ggtgagcttgccc-3′; Glu-337 sense 5′-gcatgcacaagaagg**C**gaagtccgtgctgcagggc-3′ and antisense 5′-gccctgcagcacggacttc**G**ccttcttgtgcatgc-3′; Ser-339 sense 5′-gcatgcacaagaaggagaag-**G**ccgtgctgcagggc-3′ and antisense 5′-gccctgcagcacgg**C**-cttctccttcttgtgcatgc-3′.

The PMCA2_4 M mutant, in which all the four lysines were mutated, was generated by subsequent cycles of PCR amplification using the following primers: Lys-336_338 sense 5′-ccagcatgcacaag**GC**ggag**GC**gtccgtgctgcagg-3′ and antisense 5′-cctgcagcacggcc**GC**ctcc**GC**cttgtgctgctgg-3′; Lys-344_347 sense 5′-cgtgctgcagggc**GC**gctcacc**GC**gctggctgtgcaga-3′ and antisense 5′-tctgcacagccagc**GC**ggtgagc**GC**gccctgcagcacg-3′. Mutated bases are indicated by boldface capital letters.

Immunocytochemistry Analysis—CHO cells were transfected with the different PMCA2 variants and mutants. 36 h after transfection, the cells were washed twice with PBS and fixed with 3.7% formaldehyde for 20 min. The membranes were permeabilized in 0.1% Triton X-100 for 5 min and washed with 1% gelatin (type B, from bovine skin, Sigma) in PBS. The cells were immunostained with primary antibodies against PMCA2 (2N, Sigma) at a 1:100 dilution in PBS and with secondary antibodies Alexa Fluor 594 (Molecular Probes). The images were acquired using a Zeiss Axiovert microscope equipped with a 12-bit digital cooled camera (Micromax-1300Y, Princeton Instruments Inc., Trenton, NJ) using Metamorph software (Universal Imaging Corporation, West Chester, PA).

Preparation of Membranes from CHO Cells, SDS-PAGE, and Western Blotting Analysis—Thirty six hours after transfection, CHO cells were harvested in 10 mM Tris-HCl, pH 8.0, 2 mM EDTA, 2 mM PMSF, 1 mM DTT. They were disrupted by three cycles of freeze and thaw at −80/37 °C, and the insoluble proteins were sedimented at 11,000 × *g* for 30 min (4 °C). The supernatant was discarded, and the pellet was resuspended in 5 mM Tris-HCl, pH 8.0, and 10% sucrose. Proteins were separated by 7.5% SDS-PAGE and transferred to nitrocellulose membranes. 20 μg of membrane proteins were loaded onto each lane. The sheets were probed with a rabbit polyclonal antibody 2N against PMCA2 (Sigma, diluted 1:1000). After incubation with anti-rabbit horseradish peroxidase-conjugated secondary antibodies (Santa Cruz Biotechnology, Santa Cruz, CA), the blots were developed with ECL reagents (Amersham Biosciences). The quantitative analysis was carried out by densitometric analysis using the Kodak 1D Image Analysis program

(Kodak Scientific Imaging System, New Haven, CT). Antibodies against β-tubulin or β-actin were also used to normalize the data obtained from the densitometric analyses.

Cytosolic Ca^{2+} Monitoring with Recombinant Aequorin—CHO cells were plated on 13-mm glass coverslips and transfected according to the calcium-phosphate procedure. 36 h after transfection, the cells were incubated for 3 h with 5 μM of the aequorin prosthetic group coelenterazine WT in Dulbecco's modified Eagle's medium supplemented with 1% FBS at 37 °C in a 5% CO_2 atmosphere.

After incubation with coelenterazine, the coverslips were placed in a perfused thermostated (37 °C) chamber of a luminometer positioned in close proximity to a low noise photomultiplier, with a built-in amplifier discriminator. The experiments were performed in a Krebs-Ringer medium (135 mM NaCl, 5 mM KCl, 0.4 mM KH_2PO_4, 1 mM $MgSO_4$, 20 mM Hepes, pH 7.4, at 37 °C) (KRB) supplemented with 0.1% glucose and 1 mM $CaCl_2$. The cytoplasmic Ca^{2+} concentrations were measured after addition of 100 μM inositol 1,4,5-trisphosphate-generating agonist ATP. The experiments were terminated by lysing the cells with 100 μM digitonin in a hypotonic Ca^{2+}-rich solution (10 mM $CaCl_2$ in H_2O) to discharge the remaining aequorin pool. The light signal from the discriminator was collected by a Thorn-EMI photon counting board and stored in an IBM-compatible computer for further analysis. The aequorin luminescence data were calibrated off line into [Ca^{2+}] values, using a computer algorithm based on the Ca^{2+}-response curve of wild type aequorin (22).

In Silico Analysis—The protein sequence of human PMCA2 was retrieved from the NCBI data base (accession number NP_001674) (23), and amino acid conservation was evaluated with Conseq (24). Secondary structure and disorder were predicted by a consensus approach (25) and SPRITZ (26), respectively. A consensus of three methods (Prodiv-TMHMM, HMMTOP, and PHOBIUS) was adopted to predict the transmembrane regions. A homology-derived three-dimensional structure model of human PMCA2 was constructed using the Homer-A modeling server based on the PDB structure 2agv (chain A) of sarco/endoplasmic Ca^{2+}-ATPase (SERCA1a).[3] The loop insertions in human PMCA2 were modeled using a divide and conquer method (27). The C-terminal PMCA2 CaM-binding region in complex with calmodulin was modeled using the PDB structure 2KNE as template. We used the PyMOL Molecular Graphics System (DeLano Scientific, San Carlo, CA) to map the residue positions in the protein structure and visualize the electrostatic surface calculated by the Adaptive Poisson-Boltzmann Solver tool (28).

Statistical Analysis—Data are reported as means ± S.D. Statistical differences were evaluated by Student's two-tailed *t* test for unpaired samples, with *p* value 0.01 being considered statistically significant.

RESULTS

Expression of PMCA2 Isoforms in CHO Cells—GFP-tagged PMCA2 splice variants *z/b*, *w/b*, and *w/a* were overexpressed in CHO cells. Crude membranes were prepared, and 20 μg of total proteins were separated by SDS-PAGE and blotted onto nitrocellulose filters. The filter was incubated with polyclonal antibody 2N that recognizes the PMCA2 isoform and with an anti-tubulin antibody. Fig. 2 shows that all three splice isoforms of the pump were expressed at approximately equivalent levels.

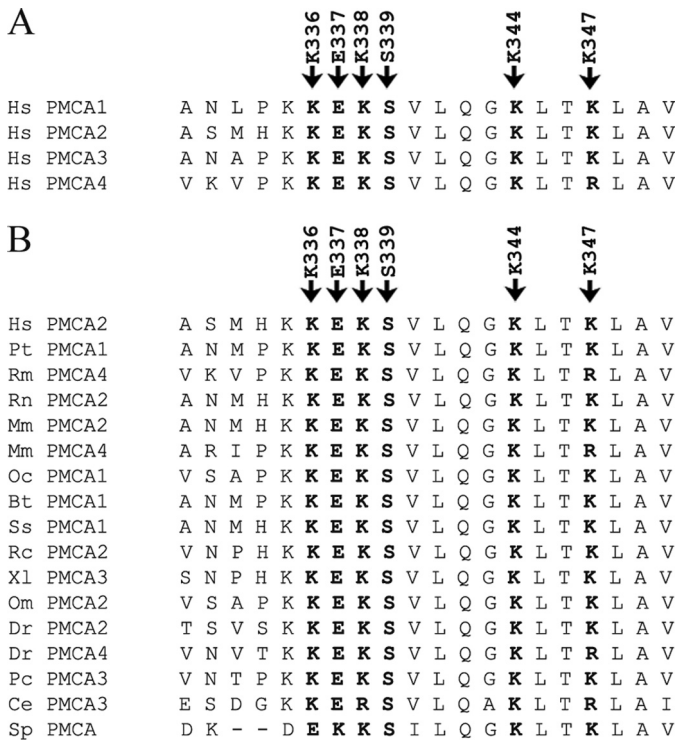

FIGURE 4. **ClustalW analysis of the A_L domain and the conservation of mutated residues.** The similarity analysis was performed using the ClustalW program. Human PMCA2 sequence (GenBank™ accession number NP_001674) is listed with other human PMCAs isoforms sequences (*A*) and with those of other species (*B*). GenBank™ accession numbers are as follows: NP_001001323 (*Homo sapiens* PMCA1), NP_068768 (*H. sapiens* PMCA3), NP_001675 (*H. sapiens* PMCA4), XP_509257 (*Pan troglodytes* PMCA1), AY928176 (*Rhesus macaque* PMCA4), NP_036640 (*Rattus norvegicus* PMCA2), AAH75643 (*Mus musculus* PMCA2), BC109173 (*M. musculus* PMCA4), Q00804 (*Oryctolagus cuniculus* PMCA1), NP_777121 (*Bos taurus* PMCA1), NP_999517 (*Sus scrofa* PMCA1), AAK11272 (*Rana catesbeiana* PMCA2), BC077905 (*Xenopus laevis* PMCA3), P58165 (*Oreochromis mossambicus* PMCA2), NP_001116710 (*Danio rerio* PMCA2), EU559285 (*D. rerio* PMCA4), AAR28532 (*Procambarus clarkia* PMCA3), AAK68551 (*Caenorhabditis elegans* PMCA3) and AAR13013 (*Stylophora pistillata*).

Ca^{2+} ATPase Activity in Microsomal Membranes—Microsomal membranes (containing plasma membrane fragments/vesicles) isolated from transfected cells were assayed in the presence of thapsigargin and oligomycin to inhibit the activity of the endogenous sarco/endoplasmic reticulum Ca^{2+}-ATPase pump and the ATP-linked Ca^{2+} uptake by mitochondrial vesicles that could possibly contaminate the microsomal preparation. Fig. 3, *A* and *D*, shows the PMCA activity in the absence of calmodulin. Both the noninserted full-length PMCA2 *z/b* variant and the *w/b* variant had higher basal activity than the inserted and truncated isoform *w/a*. The calmodulin sensitivity of each isoform was investigated at a fixed Ca^{2+} concentration in the presence of excess (200 nM) calmodulin (Fig. 3, *B* and *D*). As already shown by previous work, the *w/a* variant had reduced stimulation by calmodulin in respect to the full-length *z/b* and *w/b* variants.

[3] E. Leonardi and S. C. E. Tosatto, unpublished data.

The splicing event at site A occurs just upstream of one of the two regions responsible for the binding of acidic phospholipids. The first two spliced exons of PMCA2 encode a relatively hydrophobic stretch of amino acids positioned amid a highly charged region, suggesting possible effects on the overall interaction of the first cytosolic loop of the pump with acidic phospholipids. The response of the three pump variants *z/b*, *w/b*, and *w/a* to phosphatidylserine was thus compared. Fig. 3, *C* and *D*, shows that isoforms *z/b* and *w/b* had the same response, implying that the A_L acidic phospholipid binding domain was not affected by the site A insert. Surprisingly, however, the *w/a* variant, which has the phospholipid binding domain contiguous to the site A insert but lacks about half of the C-terminal phospholipid binding domain, was completely insensitive to phosphatidylserine; the response of the full-length variants of the pump (variants *b*) was over 5-fold higher than that of the truncated *w/a* variant. The finding thus suggests a predominant role of the C-terminal phospholipid binding domain in the response to acidic phospholipids.

Mutations in the N-terminal (A_L) Phospholipid Binding Domain—Mutational experiments on the phospholipid binding domains were performed to further explore the molecular mechanism of the activation of the pump by acidic phospholipids.

As for the possible mechanism of acidic phospholipid stimulations, in the case of the binding sequence in the C-terminal calmodulin binding domain, it was reasoned that the headgroups of positively charged residues could be neutralized by acidic phospholipids, weakening the autoinhibitory intramolecular interaction of the C-terminal tail of the pump with its receptor sites in the main body of the molecule. The study of the phospholipid binding domain in the C-terminal region was limited to comparison of the *a* variant

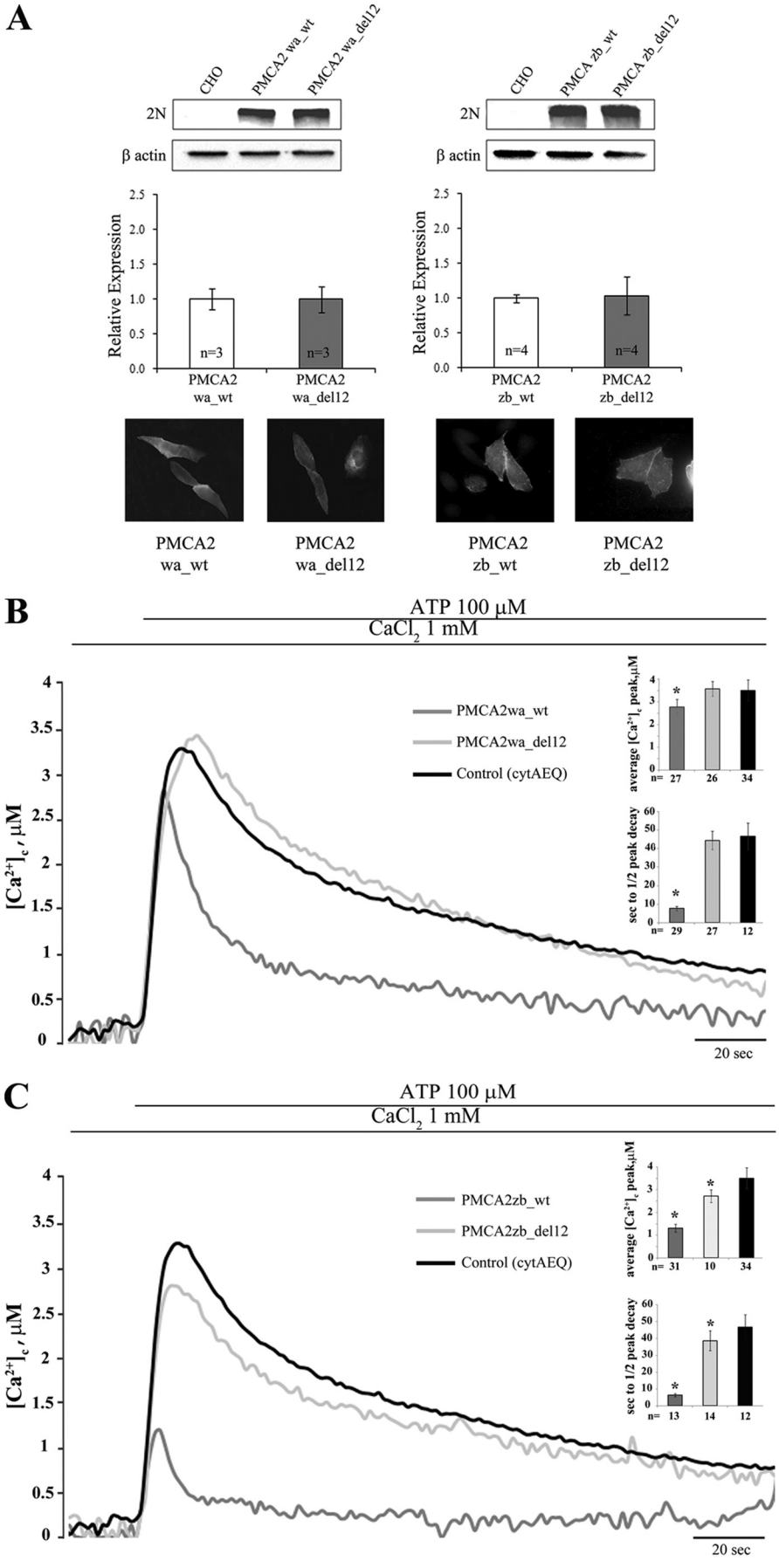

(in which the splicing truncation removes about half of the CaM binding domain and, presumably, affects the binding of acidic phospholipid binding domain) with the full-length *b* variant. No mutations were introduced in the full-length C-terminal region of the *b* variants.

In the A_L region, structural rearrangements of the transduction (activator) and catalytic domains of the pump could occur following the binding of phospholipids that would facilitate the access of Ca^{2+} to its single high affinity site in the transmembrane sector. The four lysines in the A_L phospholipid-binding region, which are very conserved among the PMCAs isoforms (Fig. 4*A*) and in the PMCA across species (Fig. 4*B*), could form a charged bend that could easily accommodate a charged phospholipid head. It was thus decided to mutate them. It was also felt that two other well conserved residues in the A_L binding domain (Glu-337 and Ser-339, Fig. 4) could also have a role in the interaction (see below). It was thus decided to mutate them as well. It was also decided to study the effect of the deletion of the 12-residue lysine-rich stretch in the A_L domain that had been previously performed by others (29).

Generation, Expression, and Activity of PMCA2zb_del12 and PMCA2wa_del12 Mutants—The 12-residue lysine-rich stretch located in the N-terminal portion of the domain was analyzed first, as it had already been shown that the deletion of this stretch failed to affect the plasma membrane targeting of the pump (29). The effect of the deletion of region 380–391 in the *w/a* variant, which has lost at least half of the C-terminal acidic phospholipid binding domain, and of region 336–347 in the full-length *z/b* variant, which contains it, was studied in over-expressing CHO cells. The activity of the deleted variants of the expressed pump was compared with that of their respective wild type variants. Appropriate controls (Western blotting and immunocytochemistry analysis) established that the mutant pump variants were expressed at about the same levels with respect to their WT versions and were correctly delivered to the plasma membrane (Fig. 5*A*). The *PMCA2wa_del12* was expressed as a GFP fusion chimera; the fusion with GFP did not alter the targeting nor the activity of the pump (29). As reported previously (19), the *w/a* variant was much less efficient than the *z/b* variant in re-establishing resting cytosolic Ca^{2+} concentrations following the increase induced by the stimulation of the cells with the purinergic agonist ATP (*traces* in Fig. 5, *B* and *C*). The Ca^{2+} transient generated by the stimulation reflects the inositol 1,4,5-trisphosphate-mediated Ca^{2+} release from the intracellular stores but also the Ca^{2+} influx from the extracellular medium through channels activated by the depletion of the endoplasmic reticulum stores. The lowering of the Ca^{2+} peak with respect to untransfected cells reflects the ability of the overexpressed pumps to respond with a burst of activation, *i.e.* of Ca^{2+} extrusion, to the arrival of the inositol 1,4,5-trisphosphate-generated Ca^{2+} pulse. The faster clearance of the Ca^{2+} signal is thus due to increased overall pump activity. Fig. 5*B* shows the Ca^{2+} response in cells transiently transfected with the *wa_wt* and *wa_del12* variants of PMCA2. Surprisingly, the deletion of the 12 amino acids in the phospholipid binding domain completely abolished the activity of the pump (the heights of the transients were *wa_wt*, 2.77 ± 0.35 μM, $n = 27$; *wa_del12*, 3.58 ± 031 μM, $n = 26$; control (only aequorin), 3.53 ± 0.48 μM, $n = 34$). The half-time of the declining phase was 7.69 ± 1.23 s, $n = 29$, in *wa_wt*, 44.52 ± 4.99 s in *wa_del12*, $n = 27$, and 46.67 ± 7.35 s, $n = 12$ in the control (see Fig. 5*B*, *inset*). Fig. 5*C* shows pump activity in cells transiently transfected with the *wt_zb* and *zb_del12* PMCA2 variants. The 12-amino acid deletion impaired the activity of the *zb* variant as well (*zb_wt*, 1.31 ± 0.17 μM, $n = 31$; *zb_del12*, 2.72 ± 0.28 μM, $n = 10$), suggesting that the deleted residues are important to pump activity independently of splicing processes. However, at variance with the *wa_del12* variant, the *zb_del12* variant was still partially active; the height of Ca^{2+} transient was reduced with respect to control cells. This finding is also supported by the analysis of the declining phase of the Ca^{2+} traces, in which the half-time of the peak decay was 6.31 ± 0.85 s, $n = 13$, in *zb_wt*, 38.64 ± 5.93 s in *zb_del12*, $n = 14$, *versus* 46.67 ± 7.35 s, $n = 12$, in the control, $p < 0.01$ (see Fig. 5*C*, *inset*).

Generation, Expression, and Activity of PMCA2 z/b Variants Harboring Single Lys Mutations in the 336–347 Domain—Single amino acids mutants of the PMCA2 *z/b* pump were generated by replacing individual lysines in the 12-residue sequence (336–347 domain). Five mutants were generated as follows: PMCA2*zb_K336A*, PMCA2*zb_K338A*, PMCA2*zb_K344A*, PMCA2*zb_K347A*, and one in which all four lysines were replaced with alanines, PMCA2*zb_4M*. The positions of the mutated lysines in the sequence are shown in Fig. 4. The level of expression of all mutants and their correct delivery to the plasma membrane were checked and found to be equivalent (Fig. 6*A*). The single mutation of three of the four lysines impaired the activity of the pump (the heights of the peak transients induced by the stimulation were as follows: 1.50 ± 0.15 μM, $n = 12$ for PMCA2 *zb_K338A*; 1.96 ± 0.09 μM, $n = 15$ for PMCA2 *zb_K344A*; and 1.56 ± 0.22 μM, $n = 15$ for PMCA2 *zb_K347 versus* 1.31 ± 0.17 μM, $n = 31$ for the *zb_wt*, $p < 0.01$) (Fig. 6*B*, in which the Ca^{2+} transients were superimposed to that generated in cells overexpressing equivalent levels of PMCA2*zb_wt*). Fig. 6*B* shows that instead the mutation of lysine 336 (K336A) had no effect on the Ca^{2+} extruding ability of the pump; the height of the transient was 1.36 ± 0.15 μM, $n = 12$, as compared with 1.31 ± 0.17 μM, $n = 31$, in *zb_wt*-expressing cells.

The mutation of all four lysines impaired the Ca^{2+} extrusion activity of the pump. The peak height was 1.78 ± 0.16 μM, $n =$

FIGURE 5. *A,* Western blotting and densitometric analysis of the variants of the PMCA2 isoform overexpressed in CHO cells. 20 μg of crude membrane proteins from transfected CHO cells, prepared by a freeze and thaw method, were separated by SDS-PAGE as described under "Experimental Procedures" and stained with polyclonal antibody 2N. The control lane corresponds to nontransfected cells (*CHO*). The other lanes correspond to cells transfected with the WT or mutant variants of the PMCA2 pump. The *panel a*lso shows the immunocytochemistry analysis of the transfected CHO cells. The immunostaining was carried out with the 2N antibody and revealed with the secondary antibody Alexa Fluor 594. *B,* monitoring of cytosolic [Ca^{2+}] in CHO cells transfected with cytAEQ and co-transfected with cytAEQ and the WT *w/a* variant of PMCA2 isoform or deleted PMCA2*wa_del12* mutant. *C,* monitoring of cytosolic [Ca^{2+}] in CHO cells transfected with cytAEQ and co-transfected with cytAEQ and the wt *z/b* variant of PMCA2 isoform or deleted PMCA2*zb_del12* mutant. The *histograms* in *B* and *C* show the means ± S.D. of $[Ca^{2+}]_c$ peaks and of the half-time decays from the peaks. The traces are representative of at least 12 independent experiments. *, $p < 0.01$ calculated with respect to control (CHO cells transfected only with cytAEQ).

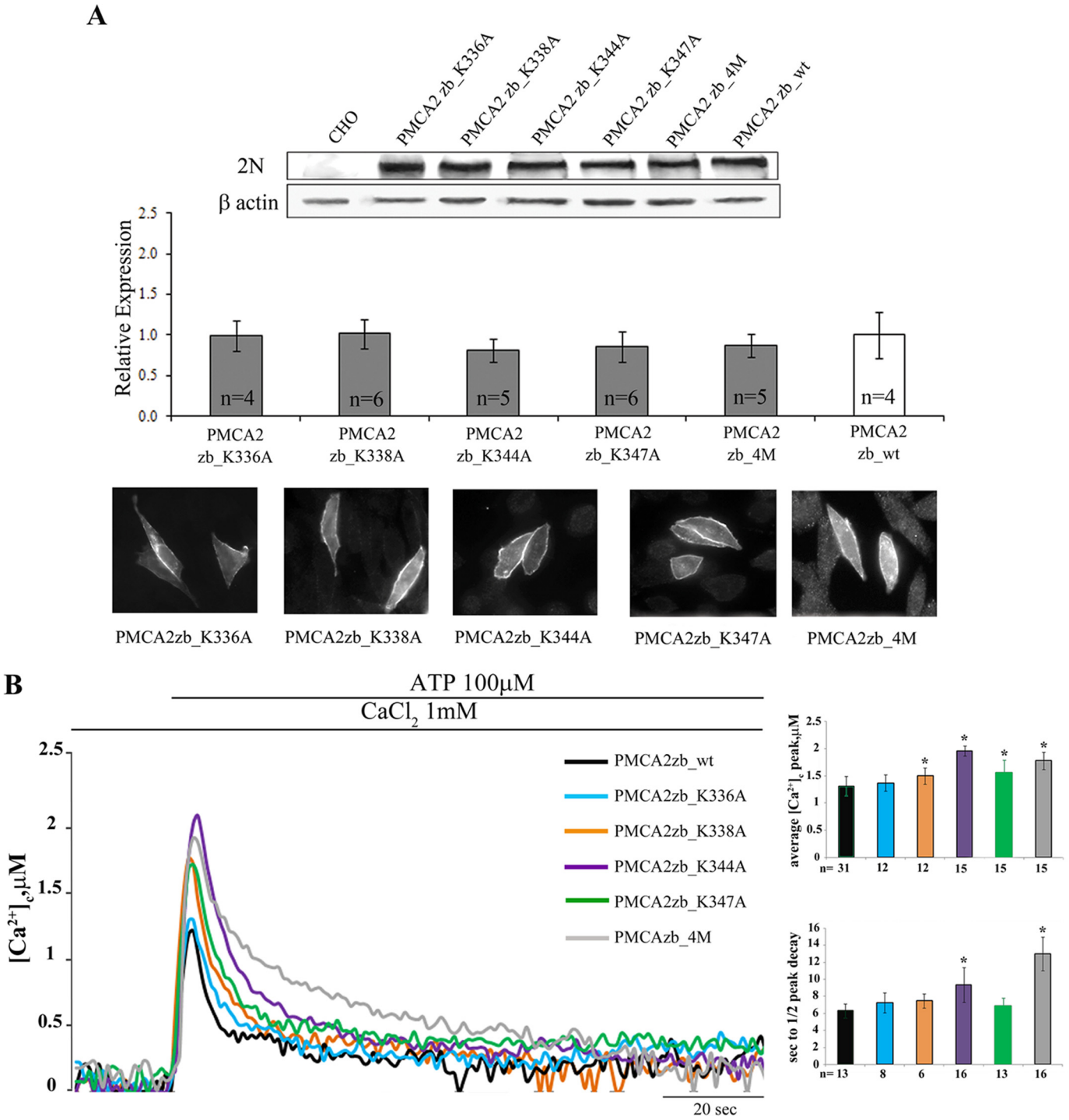

FIGURE 6. *A,* Western blotting and densitometric analysis of the Lys mutants of the PMCA2 *z/b* isoform overexpressed in CHO cells. 20 μg of crude membrane proteins from transfected CHO cells, prepared by a freeze and thaw method, were separated by SDS-PAGE as described under "Experimental Procedures" and stained with polyclonal antibody 2N. The control lane corresponds to nontransfected cells (*CHO*). The other lanes correspond to cells transfected with the WT or mutant variants of the PMCA2 pump. The *panel* also shows the immunocytochemistry analysis of the transfected CHO cells. The immunostaining was carried out with the 2N antibody and revealed with the secondary antibody Alexa Fluor 594. *B,* monitoring of cytosolic [Ca^{2+}] in CHO cells transfected with cytAEQ and co-transfected with cytAEQ and the PMCA2*zb_K336A*, PMCA2*zb_K338A*, PMCA2*zb_K344A*, PMCA2*zb_K347A*, or PMCA2*zb_4M*, alternatively. The *histograms* show the means ± S.D. of $[Ca^{2+}]_c$ peaks and of the half-time decays from the peaks. The traces are representative of at least 12 independent experiments. *, $p <$ 0.01 calculated with respect to PMCA2*zb_wt* (CHO cells transfected with wt PMCA2 *z/b* pump).

15, for PMCA2 *zb_4M versus* 1.31 ± 0.17 μM, $n = 31$, for *zb_wt*, $p < 0.01$. It also affected the ability of the pump to accelerate the declining phase of the Ca^{2+} transient trace. It did so more significantly than in the case of single lysine mutants, as shown by the *traces* and the *histograms* of Fig. 6*B*. The half-time of the declining phase was 7.25 ± 1.16 s, $n = 8$, for PMCA2*zb_K336A*; 7.5 ± 0.83 s, $n = 6$, for PMCA2*zb_K338A*; 9.37 ± 2.02 s, $n = 16$, for PMCA2*zb_K344A*; 6.89 ± 0.93 s, $n = 13$, for PMCA2*zb_K347A*; 13 ± 2 s, $n = 16$, for PMCA2*zb_4M*, and 6.31 ± 0.85 s, $n = 13$, for *zb_wt*, $p < 0.01$.

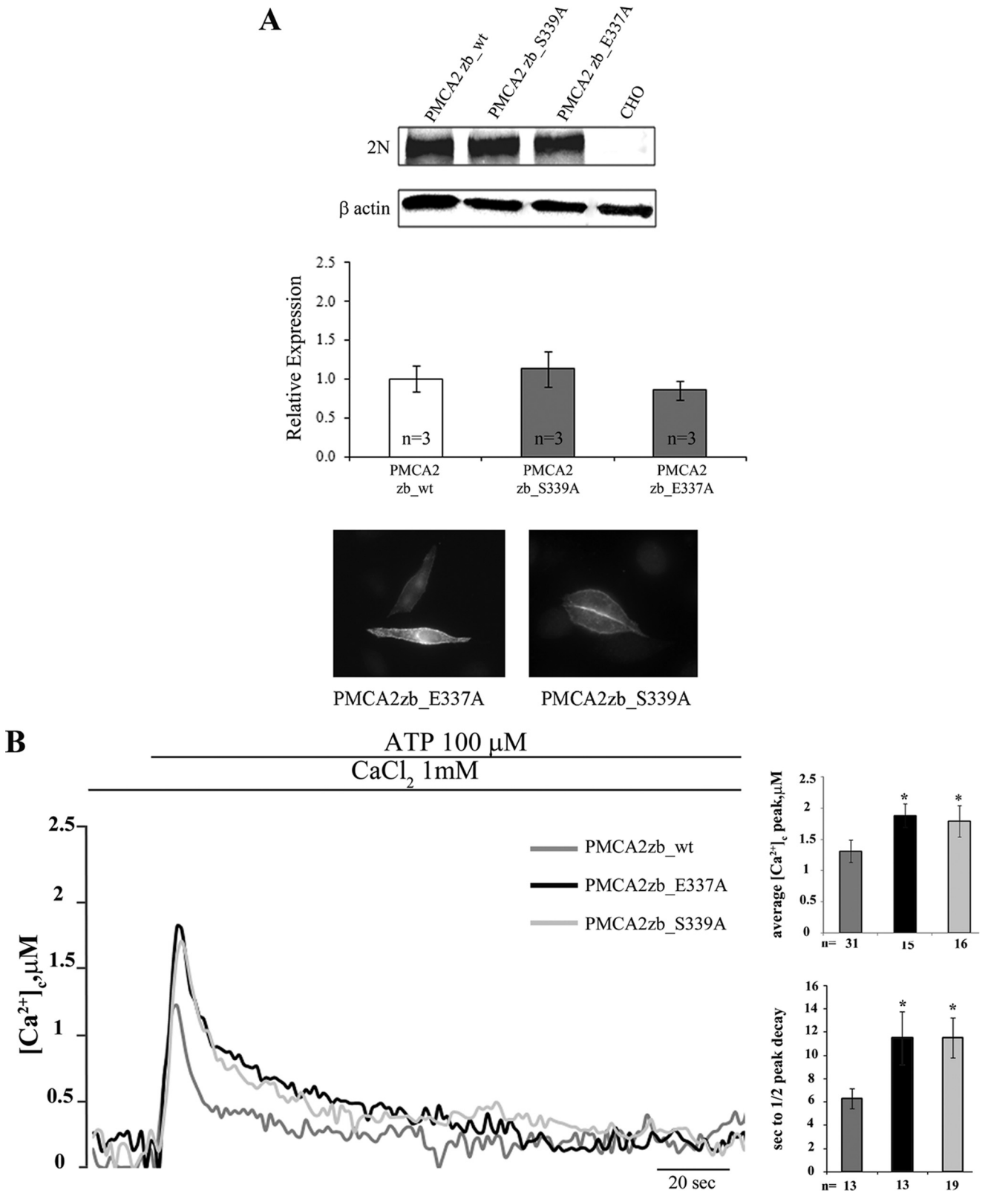

FIGURE 7. *A,* Western blotting and densitometric analysis of the Glu and Ser mutants of the PMCA2 *z/b* isoform overexpressed in CHO cells. 20 μg of crude membrane proteins from transfected CHO cells, prepared by a freeze and thaw method, were separated by SDS-PAGE as described under "Experimental Procedures" and stained with polyclonal antibody 2N. The control lane corresponds to nontransfected cells (*CHO*). The other lanes correspond to cells transfected with the WT or mutants variants of the PMCA2 pump. The panel also shows the immunocytochemistry analysis of the transfected CHO cells. The immunostaining was carried out with the 2N antibody and revealed with the secondary antibody Alexa Fluor 594. *B,* monitoring of cytosolic $[Ca^{2+}]$ in CHO cells transfected with cytAEQ and co-transfected with cytAEQ and the PMCA2*zb_E337A* or the PMCA2*zb_S339A*. The *histograms* show the means ± S.D. of $[Ca^{2+}]_c$ peaks and of the half-time decays from the peaks. The traces are representative of at least 12 independent experiments. *, $p < 0.01$ calculated with respect to PMCA2*zb_wt* (CHO cells transfected with WT PMCA2 *z/b* pump).

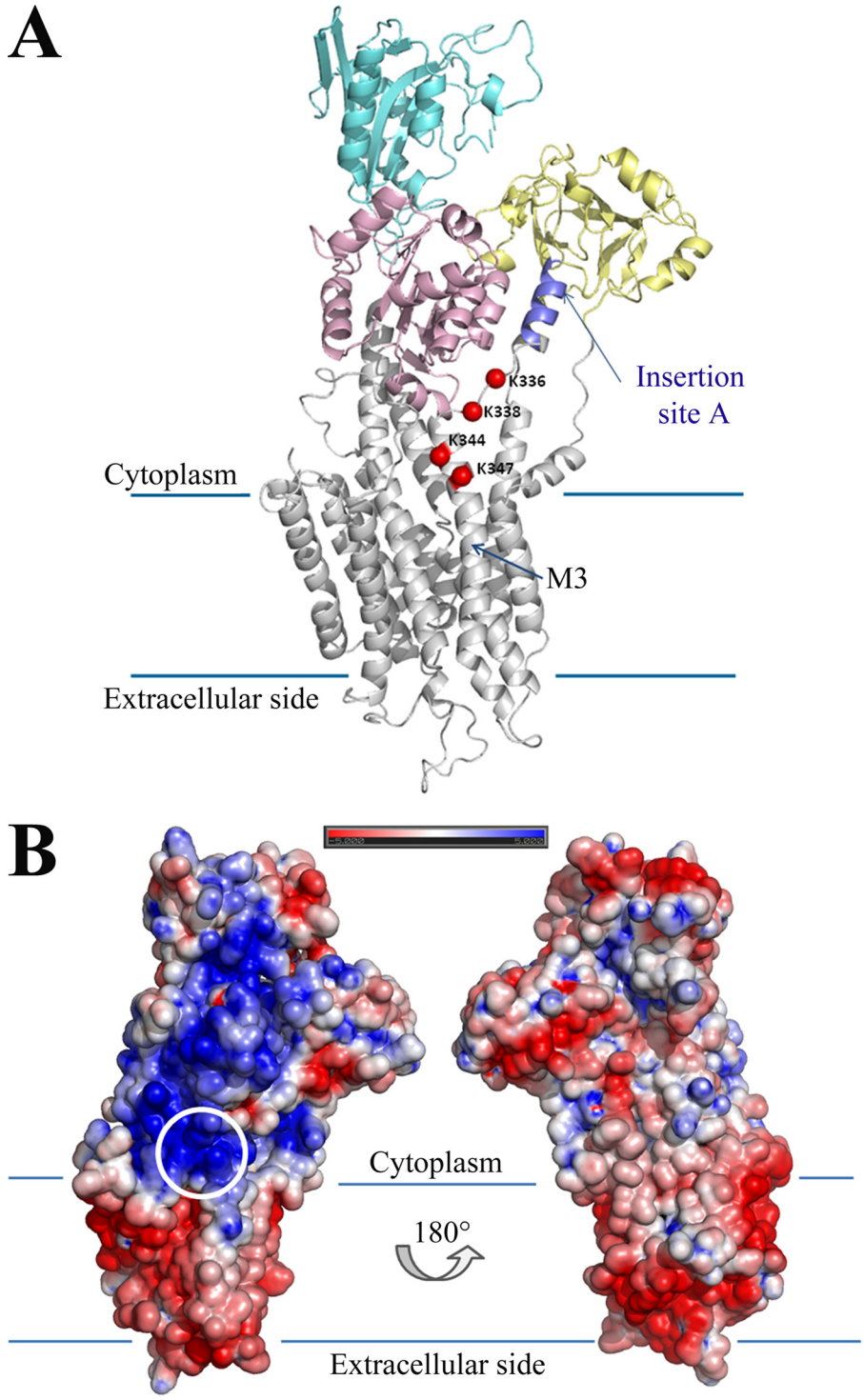

FIGURE 8. *A,* overview of the PMCA2 model, shown in schematics and color-coded for the different canonical domains, with the four mutated lysines highlighted as *red spheres*. The approximate location of the membrane limits are shown with *lines*, and the third transmembrane helix is labeled as *M3*. Note that the C-terminal part of PMCA2 from residue 1088 onward could not be modeled. Insertion site A is *highlighted*. *B,* electrostatic potential of the PMCA2 accessible surface. The structure is shown in the same orientation as in *A* and rotated around the central axis (*right*). The location of the mutated lysine residues is *circled*. Note how the area around and between the four lysines and insertion site A is the only PMCA2 region with positive potential in contact with the membrane.

Generation, Expression, and Activity of E337A or S339A PMCA2 z/b Mutants—The decision to mutate basic residues (lysines) in the 336–347 domain was dictated by the ability of the domain to bind acidic phospholipids. However, the domain also contains a conserved glutamic acid in position 337 (Glu-337) and a serine in position 339 (Ser-339) (see Fig. 4). The *in silico* analysis (see below) suggests that these residues could be involved in polar interactions with other portions of the protein. Thus, they were also mutated. Fig. 7*A* shows that PMCA2*zb_E337A* and PMCA2*zb_S339A* were expressed at levels comparable with those of the transfected PMCA2*zb_wt* variant and were correctly delivered to the plasma membrane of the transfected cells.

The Ca^{2+} measurements showed that the PMCA2*zb_E337A* and the PMCA*zb_S339A* mutants were less efficient than the PMCA2*zb_wt* variant in controlling the peak of the Ca^{2+} transient (1.88 ± 0.19 μM, $n = 15$, for PMCA2*zb_E337A*, 1.79 ± 0.25 μM, $n = 16$, for PMCA2*zb_S339A versus* 1.31 ± 0.17 μM, $n = 31$, for *zb_wt*, $p < 0.01$) (Fig. 7*B*). The mutations also severely affected the ability of the pump to restore basal Ca^{2+} levels after cell stimulation, the half-time of the peak decay being 11.52 ± 2.27 s, $n = 13$, in PMCA2*zb_E337A* and 11.26 ± 1.73 s, $n = 19$, in PMCA*zb_S339A*, as compared with 6.31 ± 0.85 s, $n = 13$, in *zb_wt*, $p < 0.01$ (Fig. 7*B*).

In Silico Analysis of the Two Phospholipid Binding Domains—Fig. 8*A* shows a schematic of the PMCA2 in which three of four lysines (Lys-338, Lys-344, and Lys-347) contained in the A_L domain are predicted to be located approximately at the membrane surface, forming a charged bend which, as already mentioned, could easily accommodate a charged phospholipid head. The electrostatic surface potential of PMCA2 (Fig. 8*B*) shows that the region surrounding the lysines, and stretching toward insertion site A, is the only positively charged region in contact with the cytoplasmic side of the membrane. Over 30 residues close to insertion site A could not be modeled; thus, the model is only approximate. However, the missing residues are likely to form a mobile flap extruding from the protein structure. Because conformational switches are required for Ca^{2+} transport, it could

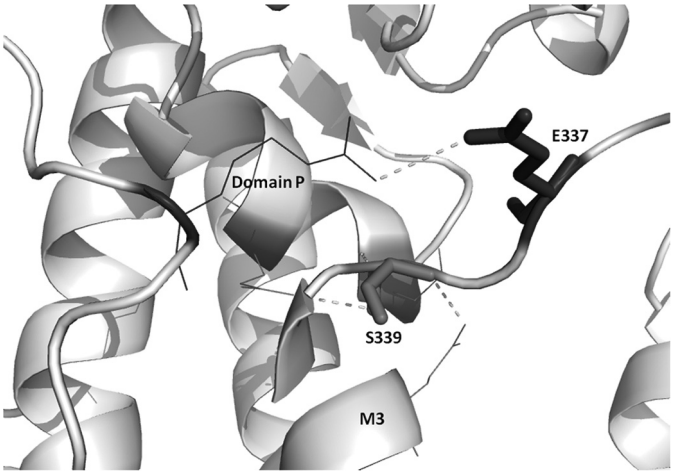

FIGURE 9. **Representation of the two residues, Ser-337 and Glu-339 (*dark gray*).** These are shown as *sticks*, and *dashed lines* indicate interatomic contacts or hydrogen bonds with neighboring residues.

be reasonably suggested that the three lysines would form a binding pocket for initial phospholipid docking. The model agrees well with the experimental findings on the importance of three of the four lysines, as well as with the effect of the 12-residue deletion. Mutation of all four lysines is likely to slow down phospholipid docking, but the positively charged area surrounding insertion site A could partially compensate for this effect.

The two other mutated residues (Glu-337 and Ser-339), are well conserved in PMCA isoforms and in the PMCA across species (see Fig. 4). The model positions glutamic acid between two lysines and exposes it to the protein surface, where it could affect other interactions of the pump. As for the serine, its polar group forms a hydrogen bond with a glutamine in the α-helix (M3) and with a glutamic acid in the α-helix of domain P (Fig. 9). Mutational disruption of hydrogen bonds may have significant structural consequences.

The C-terminal splice variant *w/a* differs from the *w/b* variant by a frameshift mutation affecting the second half of the CaM-binding region. The model generated by the structural analysis (Fig. 10*A*) shows that the PMCA2 CaM-binding region (obtained from the recently deposited NMR structure of the PMCA4 CaM-binding region (PDB code 2KNE) could form an amphiphilic α-helix with a distinctive pattern of charged and hydrophobic residues (30). In the presence of Ca^{2+} ions, CaM folds into a series of α-helices winding around the PMCA2 peptide in a head-to-tail conformation, *i.e.* the N terminus of CaM binds the C terminus of PMCA2. Ca^{2+} could induce a conformational switch through the stabilization of a stretch of negatively charged residues in a turn conformation, yielding the characteristic collapsed structure of CaM. Interestingly, the final conformation has a strongly negative charge and is stabilized through hydrophobic cages between a benzyl ring and a hydrophobic groove at the center of three CaM α-helices (Fig. 10*B*). In the model, electrostatic attraction is present, but is not crucial to stabilize the final bound conformation. Given the number of charged residues in CaM, electrostatic attraction is likely to initiate the folding process of CaM around the PMCA2-binding region. The substitution of two lysine residues in the CaM binding domain of the *w/a* variant (see sequence alignment in Fig. 10*A*) could destabilize the CaM interactions necessary to form the hydrophobic cage for proper binding, explaining the poor sensitivity to CaM of the variant.

DISCUSSION

It would be reasonable to expect that the proximity of site A of alternative splicing to the site that binds acidic phospholipids in the A_L domain could influence the sensitivity of PMCAs to acidic phospholipids. The A-site insertion could alter the overall conformation of the second cytosolic loop of the pump. It could thus change the spatial connectivity between the phospholipid binding domain and the sequence further upstream, which is involved in the intramolecular inhibitory interaction with the C-terminal calmodulin binding domain. The finding that the A-site insert is important for the targeting of PMCA pump to the apical membrane (5) underlines its importance in the general properties of the pump. The role of the A_L phospholipid binding domain has always been obscure, particularly in view of the existence of a second phospholipid binding domain in the C-terminal calmodulin binding sequence (7). One still open question is thus the comparative importance of the two phospholipid binding domains in the regulation of pump activity. Our previous studies on isoform 2 of the PMCA pump had shown differences in the activity of the various A-site splicing variants (19, 20), showing that the *w/a* variant had high basal Ca^{2+} ejection activity but failed to respond rapidly to the sudden arrival of a Ca^{2+} pulse. It had already been reported that both isoforms PMCA2b and -2a have much higher affinity for CaM than the corresponding isoforms of PMCA4, with PMCA2b having the highest affinity. They were both activated at low Ca^{2+}-calmodulin levels and had peculiarly high activity in the absence of activators (18).

The measurements of ATPase activity in microsomal membranes of transfected CHO cells have indicated that the *w/a* variant, as expected, was much less sensitive to CaM than the *z/b* and *w/b* isoforms. However, it was also less sensitive to phosphatidylserine, thus underlining the role of the CaM binding domain in the regulation of pump activity by acidic phospholipids. The finding that the *z/b* and *w/b* isoforms had the same response to phosphatidylserine stimulation had indicated that the splicing insertion upstream of the A_L phospholipid binding domain failed to modify the phospholipid sensitivity of the pump.

The analysis of the A_L 12-amino acid lysine-rich stretch, and the model derived from it, had indicated the importance of the conserved lysines in the stretch in the interaction of the phospholipid binding domain with the pump microenvironment. The deletion of the 12 amino acids could, for instance, directly affect the structure of M3, which is critical to the sarco/endoplasmic reticulum Ca^{2+}-ATPase pump binding of thapsigargin and could by analogy have special importance to PMCA as well. In the sarco/endoplasmic reticulum Ca^{2+}-ATPase pump, the segment linking M3 to the A domain is essential for the rotation of the latter and for its correct positioning in the active configuration of the catalytic site (31).

By combining the structural information on the four A_L lysines and on the C-terminal CaM-binding region, it could be proposed that the C-terminal domain of the pump that con-

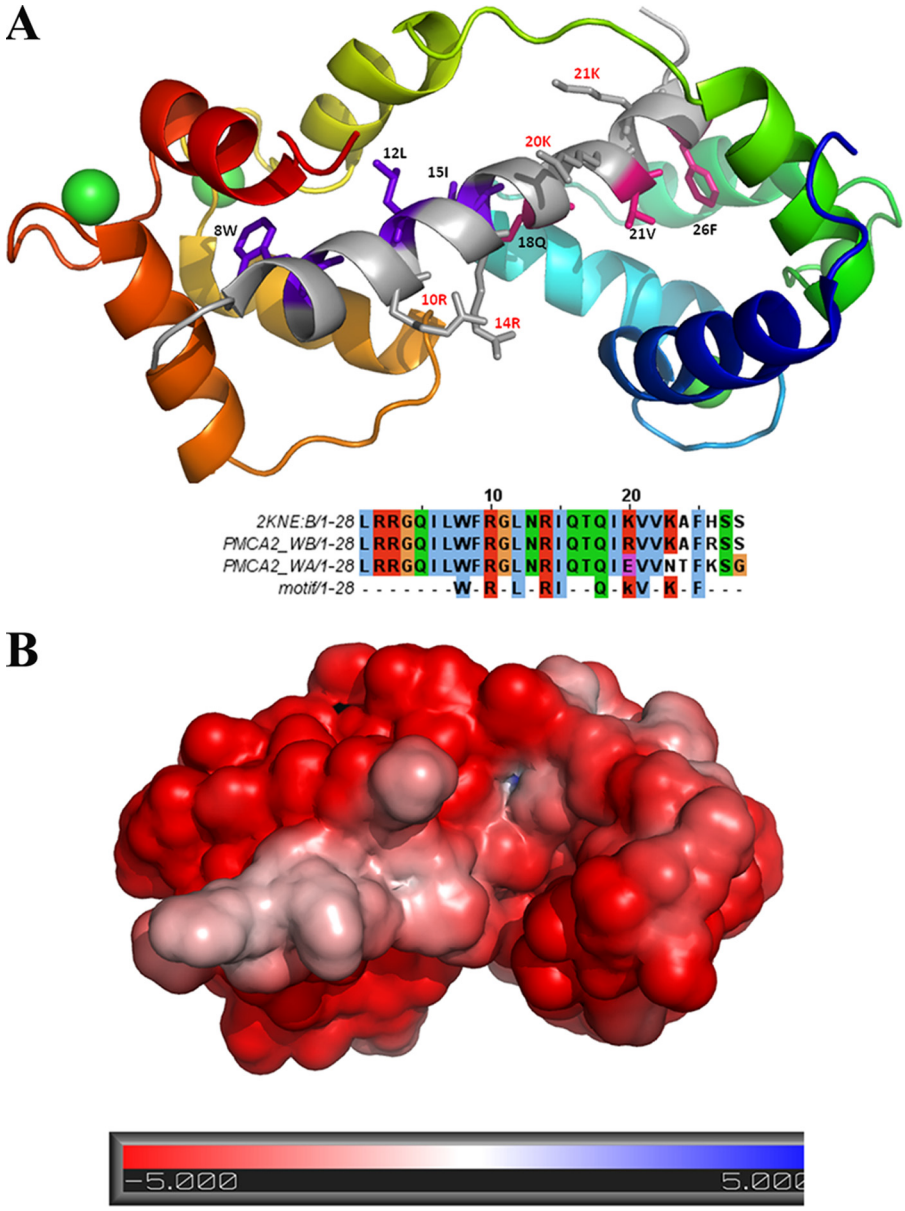

FIGURE 10. *A,* structural model of the calmodulin-binding region of PMCA2 (*top*) and relative sequence alignment (*bottom*). The amphipathic PMCA2 helix is shown in *gray* at the *center* of the structure, with residues in *purple* and *pink* defining the N- and C-terminal motifs. The calmodulin structure is shown with progressively varying color, from *blue* (N terminus) to *red* (C terminus). Ca^{2+} ions are shown as *green spheres*. The sequence alignment shows the structural template (PMCA4, PDB code 2KNE) together with two PMCA2 variants. The *last line* defines the sequence motif for calmodulin binding. Note how PMCA2 *w/a* lacks two crucial lysine residues for the second motif. *B,* electrostatic surface of the calmodulin-binding region of PMCA2 with bound CaM in the same orientation as in *A*.

tains the CaM-binding region could anchor Ca^{2+} ions to PMCA; it has indeed been shown that Ca^{2+}-binding sites are present upstream and downstream of the CaM binding domain (32). Once CaM is bound, the PMCA movements could bring the Ca^{2+} ions closer to the lysine-containing region near insertion site A through electrostatic attraction.

The finding that the deletion of the 12-residue A_L domain completely abolished the activity of the pump in the *w/a* variant, but not in the *z/b* variant in which it only reduced it, indicated that the activity of the PMCA2 *w/a* variant strongly depended on the presence of the A_L(380–391) region and possibly on the acidic phospholipid binding to it. The finding that the *w/a* variant was insensitive to PS in the microsomal membranes assay could mean that its stimulation was already maximal under these conditions, as endogenous acidic phospholipids are present in the membranes and could have saturated the PL binding domain. Further addition of PS could not further stimulate the activity of the *w/a* variant. Evidently, CaM activation is not sufficient to make the *w/a* variant as active as the *z/b* and the *w/b* variant. Thus, the difference between the activities of the *w/a* and *z/b* variants observed in the measurements performed in intact cells could be related to their interaction with acidic phospholipids, as also suggested by the ATPase activity measurements on microsomal membranes. In other words, the *z/b* variant would be more active than the *w/a* variant because of the integrity of its two acidic phospholipid-binding sites. The truncation of the protein induced by the site C splicing drastically affected the ability of the pump to bind activator phospholipids, and the deletion of the 12-residue A_L domain further compromised its activity.

Interestingly, the substitution of all four positively charged residues (lysines) reduced the Ca^{2+} extrusion ability of the pump by about the same extent as the replacement of only Lys-344, suggesting a critical role for Lys-344 in pump activity. However, the mutation of two polar residues (Glu and Ser) in the same region affected the pump activity to about the same extent, suggesting that the disruption of the possible interaction of this region of the pump with the other pump region (or with other proteins) may be as important to pump activity as the impairment of its ability to bind acidic phospholipids.

Acknowledgments—We are indebted to Dr. E. E. Strehler (Rochester, MN) for the donation of PMCA2w/a expression plasmid and to Dr. R. Wenthold (Bethesda) for the donation of PMCA2w/a_del12 expression plasmid.

REFERENCES

1. Brini, M., Coletto, L., Pierobon, N., Kraev, N., Guerini, D., and Carafoli, E. (2003) *J. Biol. Chem.* **278,** 24500–24508
2. Brini, M., and Carafoli, E. (2009) *Physiol. Rev.* **89,** 1341–1378

3. Rimessi, A., Coletto, L., Pinton, P., Rizzuto, R., Brini, M., and Carafoli, E. (2005) *J. Biol. Chem.* **280,** 37195–37203
4. Linde, C. I., Di Leva, F., Domi, T., Tosatto, S. C., Brini, M., and Carafoli, E. (2008) *Cell Calcium* **43,** 550–561
5. Chicka, M. C., and Strehler, E. E. (2003) *J. Biol. Chem.* **278,** 18464–18470
6. Xiong, Y., Antalffy, G., Enyedi, A., and Strehler, E. E. (2009) *Biochem. Biophys. Res. Commun.* **384,** 32–36
7. Brodin, P., Falchetto, R., Vorherr, T., and Carafoli, E. (1992) *Eur. J. Biochem.* **204,** 939–946
8. Heim, R., Iwata, T., Zvaritch, E., Adamo, H. P., Rutishauser, B., Strehler, E. E., Guerini, D., and Carafoli, E. (1992) *J. Biol. Chem.* **267,** 24476–24484
9. Adamo, H. P., and Penniston, J. T. (1992) *Biochem. J.* **283,** 355–359
10. Enyedi, A., Flura, M., Sarkadi, B., Gardos, G., and Carafoli, E. (1987) *J. Biol. Chem.* **262,** 6425–6430
11. Papp, B., Sarkadi, B., Enyedi, A., Caride, A. J., Penniston, J. T., and Gardos, G. (1989) *J. Biol. Chem.* **264,** 4577–4582
12. Missiaen, L., Raeymaekers, L., Wuytack, F., Vrolix, M., de Smedt, H., and Casteels, R. (1989) *Biochem. J.* **263,** 687–694
13. Missiaen, L., Wuytack, F., Raeymaekers, L., De Smedt, H., and Casteels, R. (1989) *Biochem. J.* **261,** 1055–1058
14. Pérez-Gordones, M. C., Lugo, M. R., Winkler, M., Cervino, V., and Benaim, G. (2009) *Arch. Biochem. Biophys.* **489,** 55–61
15. Pinto Fde, T., and Adamo, H. P. (2002) *J. Biol. Chem.* **277,** 12784–12789
16. de Tezanos Pinto, F., and Adamo, H. P. (2006) *FEBS Lett.* **580,** 1576–1580
17. Hilfiker, H., Guerini, D., and Carafoli, E. (1994) *J. Biol. Chem.* **269,** 26178–26183
18. Elwess, N. L., Filoteo, A. G., Enyedi, A., and Penniston, J. T. (1997) *J. Biol. Chem.* **272,** 17981–17986
19. Ficarella, R., Di Leva, F., Bortolozzi, M., Ortolano, S., Donaudy, F., Petrillo, M., Melchionda, S., Lelli, A., Domi, T., Fedrizzi, L., Lim, D., Shull, G. E., Gasparini, P., Brini, M., Mammano, F., and Carafoli, E. (2007) *Proc. Natl. Acad. Sci. U.S.A.* **104,** 1516–1521
20. Domi, T., Di Leva, F., Fedrizzi, L., Rimessi, A., and Brini, M. (2007) *Ann. N.Y. Acad. Sci.* **1099,** 237–246
21. Huang, T. G., and Hackney, D. D. (1994) *J. Biol. Chem.* **269,** 16493–16501
22. Brini, M., Marsault, R., Bastianutto, C., Alvarez, J., Pozzan, T., and Rizzuto, R. (1995) *J. Biol. Chem.* **270,** 9896–9903
23. Bairoch, A., Apweiler, R., Wu, C. H., Barker, W. C., Boeckmann, B., Ferro, S., Gasteiger, E., Huang, H., Lopez, R., Magrane, M., Martin, M. J., Natale, D. A., O'Donovan, C., Redaschi, N., and Yeh, L. S. (2005) *Nucleic Acids Res.* **33,** D154–D159
24. Berezin, C., Glaser, F., Rosenberg, J., Paz, I., Pupko, T., Fariselli, P., Casadio, R., and Ben-Tal, N. (2004) *Bioinformatics* **20,** 1322–1324
25. Albrecht, M., Tosatto, S. C., Lengauer, T., and Valle, G. (2003) *Protein Eng.* **16,** 459–462
26. Vullo, A., Bortolami, O., Pollastri, G., and Tosatto, S. C. (2006) *Nucleic Acids Res.* **34,** W164–W168
27. Tosatto, S. C., Bindewald, E., Hesser, J., and Männer, R. (2002) *Protein Eng.* **15,** 279–286
28. Baker, N. A., Sept, D., Joseph, S., Holst, M. J., and McCammon, J. A. (2001) *Proc. Natl. Acad. Sci. U.S.A.* **98,** 10037–10041
29. Grati, M., Aggarwal, N., Strehler, E. E., and Wenthold, R. J. (2006) *J. Cell Sci.* **119,** 2995–3007
30. Juranic, N., Atanasova, E., Filoteo, A. G., Macura, S., Prendergast, F. G., Penniston, J. T., and Strehler, E. E. (2010) *J. Biol. Chem.* **285,** 4015–4024
31. Toyoshima, C. (2008) *Arch. Biochem. Biophys.* **476,** 3–11
32. Hofmann, F., James, P., Vorherr, T., and Carafoli, E. (1993) *J. Biol. Chem.* **268,** 10252–10259